MCB
Journals.ASM.org

Glycogen Synthase Kinase 3 Inhibition Promotes Lysosomal Biogenesis and Autophagic Degradation of the Amyloid-β Precursor Protein

Callum Parr,[a] Raffaela Carzaniga,[b] Steve M. Gentleman,[a] Fred Van Leuven,[c] Jochen Walter,[d] and Magdalena Sastre[a]

Division of Brain Sciences, Imperial College London, London, United Kingdom[a]; Electron Microscopy Centre, Imperial College London, London, United Kingdom[b]; Department of Human Genetics, KU Leuven, Leuven, Belgium[c]; and Department of Neurology, University Bonn, Bonn, Germany[d]

Alzheimer's disease (AD) has been associated with altered activity of glycogen synthase kinase 3 (GSK3) isozymes, which are proposed to contribute to both neurofibrillary tangles and amyloid plaque formation. However, the molecular basis by which GSK3 affects the formation of Aβ remains unknown. Our aim was to identify the underlying mechanisms of GSK3-dependent effects on the processing of amyloid precursor protein (APP). For this purpose, N2a cells stably expressing APP carrying the Swedish mutation were treated with specific GSK3 inhibitors or transfected with GSK3α/β short interfering RNA. We show that inhibition of GSK3 leads to decreased expression of APP by enhancing its degradation via an increase in the number of lysosomes. This induction of the lysosomal/autophagy pathway was associated with nuclear translocation of transcription factor EB (TFEB), a master regulator of lysosomal biogenesis. Our data indicate that GSK3 inhibition reduces Aβ through an increase of the degradation of APP and its carboxy-terminal fragment (CTF) by activation of the lysosomal/autophagy pathway. These results suggest that an increased propensity toward autophagic/lysosomal alterations in AD patients could have consequences for neuronal function.

The Ser/Thr kinase glycogen synthase kinase 3 (GSK3) has been shown to be a key regulator in the molecular pathogenesis of Alzheimer's disease (AD). The two isozymes of GSK3, α and β, display nearly identical sequences in their kinase domains, but not much is known about their isoform-specific function (17).

GSK3 activity might be increased in AD through changes in its phosphorylation state as well as expression levels, although direct evidence for this is still limited at present (4, 22). GSK3 has been proposed to contribute to both neurofibrillary tangles and amyloid plaque formation. This is based on evidence that GSK3 phosphorylates protein tau and also amyloid precursor protein (APP), thereby promoting Aβ production (3). GSK3β transgenic mice have impaired long-term potentiation (LTP) in CA1, while the induction of LTP appears to decrease kinase activity as indicated by phosphorylation of Ser9 (13, 14). In addition, tyrosine phosphorylation of GSK3 is increased in AD transgenic mice early in life by soluble amyloid species (38). Interestingly, exposure of hippocampal neurons to Aβ has been shown to increase GSK3β activity (36). As active GSK3β triggers not only phosphorylation of tau but also other events that could contribute to cell death, a major part of AD pathology could result from increased GSK3 activity.

On the other hand, treatment with LiCl, a well-known and widely used but nonspecific GSK3 inhibitor in cultured neuronal cells and Tg2576 mice, resulted in different outcomes, from reduced Aβ40 and Aβ42 loads (23, 34, 35) to increased Aβ generation (6, 8). A recent study treating the double transgenic APP/Tau mouse model with a novel specific GSK3 inhibitor resulted in lower levels of tau phosphorylation, decreased Aβ deposition and plaque-associated astrocytic proliferation, neuronal protection, and prevention of memory deficits (31). Combined data point to a damaging cycle of amyloid generation and GSK3 activation, but the molecular mechanisms by which GSK3 affects the formation of Aβ and neurofibrillary tangles remain unknown.

In this study, our aim is to define the molecular and cellular basis for GSK3 effects in APP processing. We have found that GSK3 affects the degradation of APP and its carboxy-terminal fragments (CTFs) by inducing lysosomal biogenesis and consequently altering Aβ generation. This potential neuroprotective effect of GSK3 inhibition in AD is relevant in a disease that is characterized by autophagy dysfunction (21).

MATERIALS AND METHODS

Reagents and antibodies. Antibodies used were 6E10 (against Aβ1-16) from Covance; 4G8 (against Aβ17-24) from Covance; 140 (against the carboxy terminus of APP) (described earlier [37]); 5313 (against the N terminus of APP), a kind gift from Christian Haass (Munich University); and monoclonal anti-β-actin, -LAMP-1, and -LC3 antibodies from Abcam. Antibodies against FLAG, p62, transcription factor EB (TFEB), and ATG5 were purchased from Sigma. Anti-beclin-1 (anti-BEC1) antibody was purchased from BD Biosciences. Monoclonal GSK3α/β was from Biosource. Tissue culture reagents were obtained from Invitrogen. GSK3 inhibitors VIII and XI were obtained from Calbiochem. PS1 proteasome inhibitor was from Zymed Laboratories. 3-Methyladenine (3-MA), MG132, and all other chemicals were purchased from Sigma.

Cell culture. A murine neuroblastoma cell line stably transfected with the APP-695 Swedish mutation (K595N/M596L) was used and is referred to here as N2asw (provided by Gopal Thinakaran, University of Chicago). Cells were maintained in a selective and undifferentiated state using the antibiotic G-418 at a final concentration of 0.2 mg/ml in Dulbecco's mod-

Received 10 July 2012 Returned for modification 9 August 2012
Accepted 20 August 2012
Published ahead of print 27 August 2012
Address correspondence to Magdalena Sastre, m.sastre@imperial.ac.uk.

doi:10.1128/MCB.00930-12

ified Eagle's medium (DMEM) and OPTI-MEM (GIBCO) supplemented with 5% fetal bovine serum (FBS) and penicillin-streptomycin.

Chinese hamster ovary (CHO) cells inducibly expressing the C-terminal fragment of APP (APP-CTF) (C99) were obtained from Satoru Funamoto (Doshisha University, Japan). Cells were cultured in F12 medium containing 10% FBS, penicillin-streptomycin, and 250 μg/ml zeocin. For β-CTF expression, cells were incubated overnight with 1 μg/ml tetracycline. HEK-293 cells stably transfected with the LC3-green fluorescent protein (LC3-GFP) construct were obtained from Sharon Tooze (Cancer Research UK, London, United Kingdom) (7). Cells were grown in DMEM supplemented with 10% FBS and penicillin-streptomycin. All cell lines were grown in a 5% CO_2 incubator at 37°C.

Cells were treated with two cell-permeable, isotype-specific inhibitors (Calbiochem GSK3 inhibitors VIII and XI) and with LiCl, a nonspecific GSK3 inhibitor (Sigma). The Calbiochem inhibitors were dissolved in dimethylsulfoxide (DMSO) and used at the concentrations stated in the figures. To verify the inhibition of GSK3 and to determine the appropriate concentrations of GSK3 inhibitors to be used in our assay, we previously proved that the levels of β-catenin expression were increased by incubation with these inhibitors by Western blotting of nuclear fractions of N2asw cells (data not shown).

Cells were transfected using the standard calcium phosphate method with Fugene (Roche) or Lipofectamine 2000 (Invitrogen). The following plasmid constructs were used: GFP-LC3 (from Stefan Grimm, Imperial College, London, United Kingdom) and TFEB cDNA (from Andrea Ballabio, Telethon Institute of Genetics and Medicine, Naples, Italy). Short interfering RNA (siRNA) for GSK3α/β was obtained from Cell Signaling, BEC1 siRNA was purchased from Qiagen, and TFEB siRNA and ATG5 siRNA were from Dharmacon.

Western blotting. Cell lysates and brain homogenates were extracted with radio immunoprecipitation assay buffer (1% Triton X-100, 1% sodium deoxycholate, 0.1% SDS, 150 mM NaCl, and 50 mM Tris-HCl, pH 7.2) supplemented with Roche Complete protease inhibitor cocktail. Equal amounts of protein (20 to 50 μg) samples were separated in SDS-PAGE gels, followed by immunoblotting with primary antibodies, and were detected with horseradish peroxidase (HRP)-conjugated secondary antibody in 5% nonfat dried milk in Tris-buffered saline with Tween (TBST). Membranes were developed using ECL (GE Amersham, United Kingdom) reagents and Hyperfilm ECL autoradiography film in an automated developer from Konica (SRX 101A). The intensity of the bands was quantified by densitometric scanning with ImageJ (NIH) and normalized to β-actin.

Determination of secreted Aβ and APP ectodomain. Soluble APP (sAPP) and Aβ secreted into the medium were obtained by harvesting the medium from N2asw cells. The volume of medium used was adjusted to protein concentrations measured in total cell lysates. An aliquot of the medium was run on a NuPage 4 to 12% Tris-glycine gel (Invitrogen), or Aβ was pulled down overnight at 4°C using Sepharose-protein A (Zymed) and 4G8, a monoclonal antibody recognizing amino acids 17 to 42 of human Aβ (Covance). Samples were then loaded in NuPage 4 to 12% Tris-glycine gels and transferred onto nitrocellulose membranes. The membrane was boiled in 1× phosphate-buffered saline (PBS) for 5 min, blocked with nonfat milk, and incubated with 6E10 antibody (a monoclonal antibody recognizing amino acids 1 to 17 of human Aβ; Covance) at 1/1,000. Total APPs were detected with antibody 5313 against the N terminus of APP. Membranes were incubated with HRP-conjugated secondary antibody in 5% nonfat dried milk in TBST and developed using ECL (GE Amersham, United Kingdom).

Subcellular fractionation. Cultured N2asw cells were mechanically broken in hypotonic buffer (10 mM Tris, 1 mM EDTA, 1 mM EGTA) with Roche Complete Mini protease inhibitor cocktail. Samples were then centrifuged at 5,000 rpm for 5 min. The supernatant containing the membrane and cytosol fractions was then centrifuged for 45 min at 13,000 rpm at 4°C.

Analysis of APP CTFs. Membranes were separated by electrophoresis using 4 to 12% NuPage gels, and the CTFs were analyzed by immunoblotting with antibody 140 and developed as detailed earlier (30).

Enzymatic activity. The enzymatic activity of α-secretase was measured by a fluorimetric reaction (R & D Systems) using a fluorimeter (Spectramax Gemini) using approximately 75 μg of protein lysate per well (18).

Electron microscopy. N2asw cells incubated on coverslips were washed thrice in serum-free DMEM and fixed in 4% paraformaldehyde and 1% glutaraldehyde in 0.1 mol/liter sodium cacodylate buffer (pH 7.2) overnight at room temperature. Following fixation, coverslips containing cells were treated with reduced 1% osmium followed by 1% tannic acid. Samples were processed for en face embedding in epon resin. Ultrathin sections were collected from a depth of approximately 2 μm, stained with 2% aqueous solution of uranyl acetate and Reynold's lead citrate, and then observed using a transmission electron microscope (Tecnai G2 Spirit; FEI). Images were captured on a digital camera (Eagle; FEI). The number of lysosomes per cell was counted for at least 30 cells per condition in images taken at a magnification of × 67,900 (64 mm^2).

Immunocytochemistry. N2asw and HEK-293 cells were seeded on glass coverslips and treated with inhibitor VIII overnight. For immunocytochemical detection of APP and lysosomes, antibodies 140 and LAMP1 were used. Briefly, coverslips were blocked in 3% bovine serum albumin (BSA) in 0.025% saponin. Primary antibodies were anti-APP (140) at 1/500 and anti-LAMP1 at 1/200, and they were incubated for 1 h at room temperature (RT) in 1% BSA–0.025% saponin. After five 5-min washes, Alexa Fluor secondary antibodies (488 and 594) were incubated for 1 h at RT in 1% BSA–0.025% saponin. For TFEB staining, cells were fixed in methanol. Cells were counterstained with 4′,6-diamidino-2-phenylindole (DAPI) and mounted with ProLong (Invitrogen). Z-stacks were captured on a Leica LAS AF SP5 confocal microscope with a 63× optical oil immersion lens and 2.5× digital zoom with a sequential scan between channels. Briefly, 5 randomly selected fields were captured per treatment and analyzed using ImageJ and the Imaris 7.3.0 CoLoc plugin.

Lysotracker staining. Organelles with low internal pH were labeled by Lysotracker Red DN-99 (Invitrogen) to a final concentration of 75 nM for 2 h. This medium was aspirated and washed once quickly in PBS to remove unbound Lysotracker and finally fixed in 2% paraformaldehyde (PFA) for 15 min. Coverslips were counterstained with DAPI and mounted in ProLong antifade (Invitrogen) and left to cure overnight before sealing. As an internal control, bafilomycin A1 was used (see Fig. 5A).

Pulse-chase experiments. Pulse-chase experiments were performed as described previously (29). N2asw cells were starved in methionine-free medium, pulsed in 20 μM [^{35}S]methionine (PerkinElmer and ICIS) for 20 min, and chased for up to 8 h with DMEM with excess methionine. Cell lysates were immunoprecipitated with antibody 6E10 and run in 10% SDS gels. Gels were dried at 85°C, and the signal was enhanced with 1 M sodium salicynate. Gels were exposed to Amersham Hyperfilm MP (GE Healthcare). APP levels in cell lysates were quantified by densitometric scanning with ImageJ (NIH) and calculated as the percentage of expression for each time point relative to that at time point 0.

Statistics. Data were statistically analyzed with GraphPad Prism 5 by using either one-way analysis of variance (ANOVA) (followed by either a Dunnett's test when referring to the control only or Tukey's *post hoc* test otherwise) or the Student *t* test.

RESULTS

Effects of GSK3 inhibition on Aβ generation. To confirm whether GSK3 affects Aβ generation, we measured Aβ levels by Western blotting in media from N2asw cells incubated in the absence or presence of various GSK3 inhibitors. The concentrations used were based on published reports to avoid cell toxicity (2). We observed a significant decrease in Aβ by incubation with the specific commercial GSK3 inhibitors VIII and XI (Fig. 1A). In con-

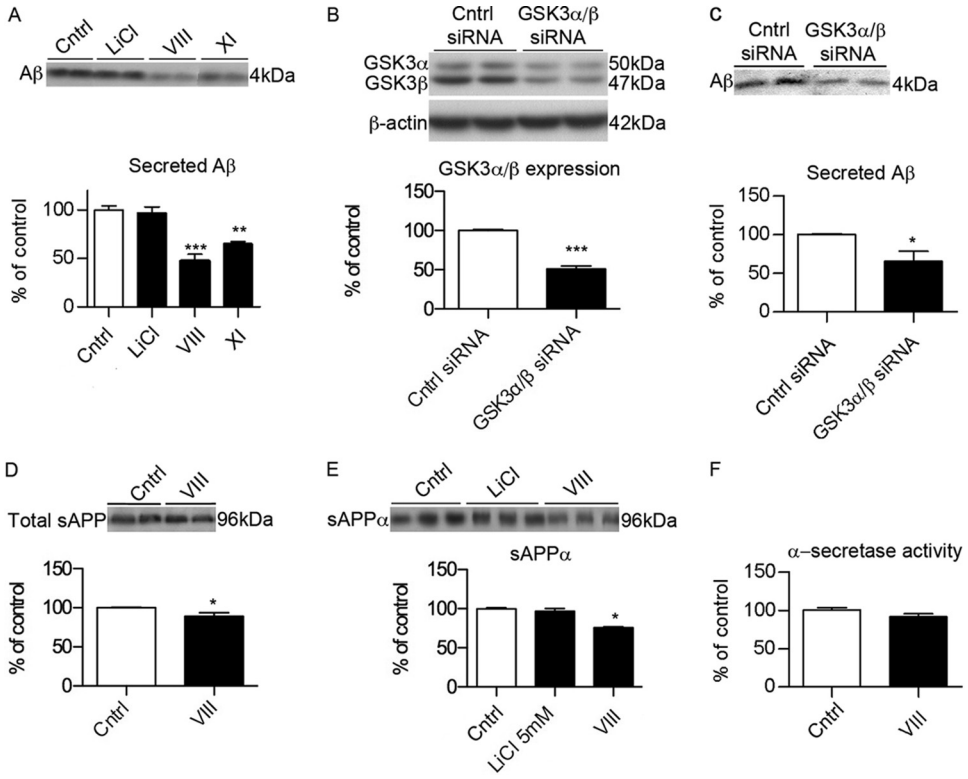

FIG 1 GSK3 inhibition reduces Aβ generation independently of α-secretase. (A) Representative Western blot and quantification of secreted Aβ (4 kDa) in media from N2asw cells treated overnight with vehicle (DMSO) or various GSK3 inhibitors, including inhibitors VIII (5 μM) and XI (10 μM; Calbiochem) and lithium chloride (20 mM) ($n = 12$). Cntrl, control. (B) Representative Western blot of GSK3α/β showing reductions in GSK3 expression after transfection with GSK3α/β siRNA (10 nM). (C) Secreted Aβ was also reduced in media from cells transfected with GSK3α/β siRNA ($n = 9$). (D) Total sAPP in media from cells treated with GSK3 inhibitor VIII (5 μM) ($n = 9$). (E) Levels of the secreted sAPPα (96 kDa) fragment were determined in media from cells treated with GSK3 inhibitors, including inhibitors VIII (5 μM) and LiCl (5 mM) ($n = 18$). (F) Enzymatic activity of α-secretase was monitored by a commercial fluorometric assay in membrane preparations from N2asw cells using GSK3 inhibitor VIII (5 μM) ($n = 9$). Bars represent means ± standard errors of the means (SEM). Asterisks represent significant differences between control and treated cells (determined by one-way ANOVA, Tukey's *post hoc* test, or Student's *t* test). *, $P \leq 0.05$; **, $P \leq 0.01$; ***, $P \leq 0.001$.

trast, LiCl did not reduce Aβ generation. GSK3α/β knockdown by siRNA (Fig. 1B) confirmed the reduction in Aβ generation observed with the specific inhibitors (Fig. 1C).

We then determined whether GSK3 inhibition affected α-secretase activity by measuring the levels of soluble APPα (sAPPα) in media. Inhibition of GSK3 by inhibitor VIII led to a significant decrease in total sAPP (Fig. 1D), in particular sAPPα (Fig. 1E). However, the activity of α-secretase measured by a fluorescence assay did not show any changes (Fig. 1F), which indicates that the reduction of sAPPα is due to a decrease in the substrate (total full-length APP) rather than a change in α-secretase activity.

GSK3 affects the levels of full-length APP. Because GSK3 inhibition affects the secretion of sAPPα, we determined whether the reductions in sAPPα and Aβ also involved changes in its precursor protein, APP, by measuring the expression of full-length APP in cell lysates from N2asw cells. Western blotting experiments using an antibody against the carboxy terminus of APP demonstrated a reduction in the expression of full-length APP in cells incubated with the GSK3 inhibitor VIII (Fig. 2A). The same results were observed in cells transfected with GSK3α/β siRNA (Fig. 2B). To investigate whether the downregulation of APP was a consequence of decreased transcription, experiments were performed in the presence of actinomycin D (a transcriptional inhibitor), which showed further reductions in APP levels in the presence of GSK3 inhibitor (Fig. 2C), indicating that the effect of GSK3 inhibition on APP was indeed independent of transcriptional regulation. In addition, semiquantitative PCR analysis was performed, demonstrating no changes in APP mRNA levels (data not shown).

We then examined whether GSK3 inhibition caused any alteration in the stability of APP by pulse-chase experiments. Cells transfected with GSK3α/β siRNA showed a more rapid APP reduction than control cells (Fig. 2D). Therefore, these results indicate that GSK3 inhibition influenced the APP degradation rate (Fig. 2D).

We thus investigated the possibility that GSK3 activity stimulates an alternative, proteasome-dependent processing pathway of APP. N2asw cells were incubated with GSK3 inhibitors in the presence or absence of the proteasome inhibitor MG132 or PS1. Because both inhibitors did not completely abolish the effect of GSK3 inhibition, we concluded that proteasomal degradation was not entirely responsible for the effects of GSK3 on APP degradation (Fig. 2E and F).

GSK3 inhibition affects the degradation of APP via autophagy. We then explored the hypothesis that GSK3 inhibition

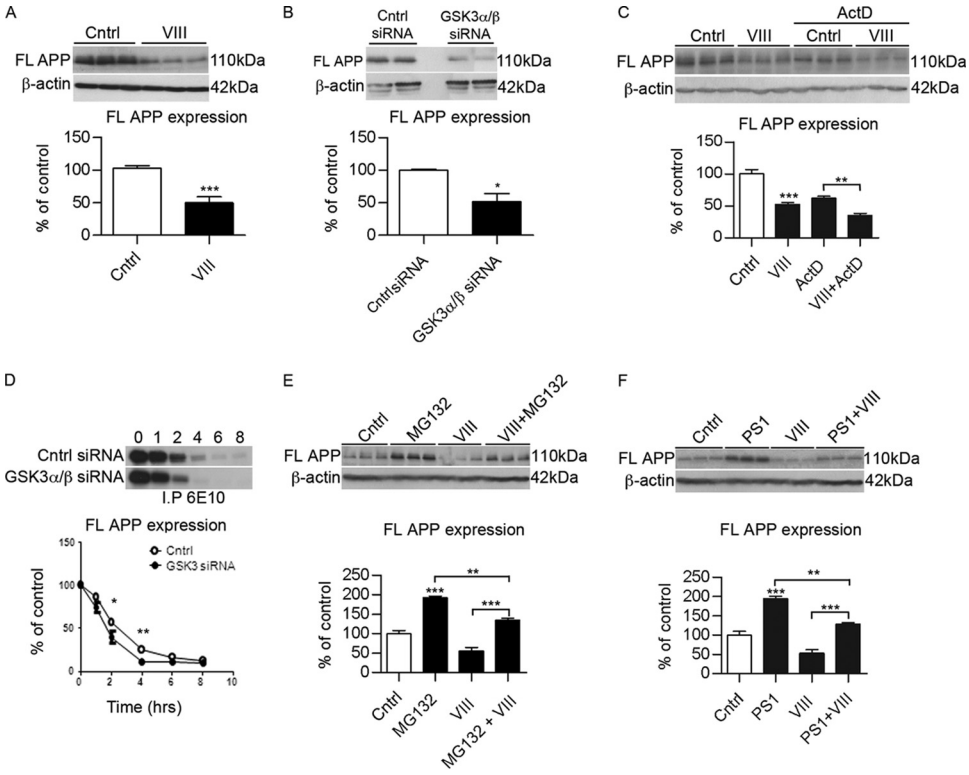

FIG 2 Inhibition of GSK3 affects the stability of full-length APP. (A) Representative Western blots and quantification of APP protein expression levels in N2asw cells treated with GSK3 inhibitor VIII (5 μM) ($n = 9$). (B) Representative Western blots and quantification of APP protein expression in N2asw cells transfected with GSK3α/β siRNA ($n = 9$). (C) Representative Western blots and quantification of APP protein expression in the presence of actinomycin D (1 μg/ml) shows a decrease in the presence of inhibitor VIII ($n = 3$). (D) Pulse-chase analysis of N2asw cells transfected with GSK3α/β siRNA. Cells were labeled with [^{35}S]methionine for 10 min and chased for the indicated time periods. APP was immunoprecipitated from cell lysates using 6E10 antibody ($n = 4$). (E) Representative Western blots and quantification of APP protein expression levels in N2asw cells treated with GSK3 inhibitor VIII (5 μM) with or without the proteasomal inhibitor MG132 (50 μg/ml) overnight ($n = 9$). (F) Representative Western blots and quantification of APP protein expression levels in N2asw cells treated with GSK3 inhibitor VIII (5 μM) with or without the proteasomal inhibitor PS1 (10 μg/ml) overnight ($n = 6$). Bars represent means ± SEM. Asterisks represent significant differences between control and treated cells (determined by one-way ANOVA, Tukey's *post hoc* test, or Student's *t* test). *, $P \leq 0.05$; **, $P \leq 0.01$; ***, $P \leq 0.001$.

favors APP degradation via the autophagy pathway. The effects of GSK3 on autophagy induction have been highly controversial (12, 25, 27, 28). Therefore, to determine whether GSK3 inhibition affected autophagy formation, we next incubated N2asw cells transfected with a LC3-GFP construct with GSK3 inhibitor VIII. LC3 is a selective marker for autophagy, which appears diffuse in normal conditions (LC3-I) and becomes punctate when it is lipidated and cleaved to form LC3-II that is associated with membranes of autophagy (19). As shown in Fig. 3A, inhibition of GSK3 increased the formation of LC3-positive puncta. To support these data, a stable HEK-293 cell line with LC3-GFP was used, and it exhibited the same effects as those of N2asw cells (Fig. 3B). Quantification of LC3-II puncta in HEK-293 cells showed a significant increase by GSK3 inhibition (Fig. 3B). To further validate these results, N2asw cells were incubated with increasing concentrations of GSK3 inhibitor VIII. Cell lysate proteins were separated by gel electrophoresis and blotted with anti-LC3 antibodies (Fig. 3C). Quantification of the LC3-I (18 kDa) and LC3-II (16 kDa) bands showed that N2asw cells respond to serum deprivation by the formation of LC3-II, and that GSK3 inhibitor VIII treatment is associated with increased conversion of LC3-I into LC3-II (Fig. 3C). To determine whether inhibitor VIII-induced accumulation of LC3-II is caused by enhanced formation of autophagic vacuoles or the blockage of autophagic vacuole degradation, we treated cells with inhibitor VIII in the absence or presence of the inhibitors of lysosomal proteolysis, leupeptin (200 μM) and NH_4Cl (20 mM), for 4 h. As shown in Fig. 3D, LC3-II levels were further accumulated in the presence of lysosome protease inhibitors, indicating an enhancement of the autophagy flux (20). These results were also supported when the degradation of p62, another protein whose levels are decreased with increased autophagy flux, was drastically reduced upon GSK3 inhibitor application (Fig. 3E).

We then tested whether or not the effect of GSK3 on APP is maintained under conditions in which autophagy is inhibited. Cells incubated in the presence of the autophagy inhibitor 3-methyladenine (3-MA) partially reversed the effect of the GSK3 inhibitor on the expression of full-length APP (Fig. 4A). To further advance our understanding of the role of autophagy in the degradation of APP in response to GSK3 inhibition, we studied the consequences of autophagy disruption by treating N2asw cell cultures with BEC1 siRNA. An increase in APP expression was detected in BEC1 knockdown N2asw cells (Fig. 4B), suggesting that APP degradation involves autophagy. In addition, BEC1 deficiency prevented the effect of GSK3 inhibition on APP degradation (Fig. 4B). This conclusion is supported by the finding that

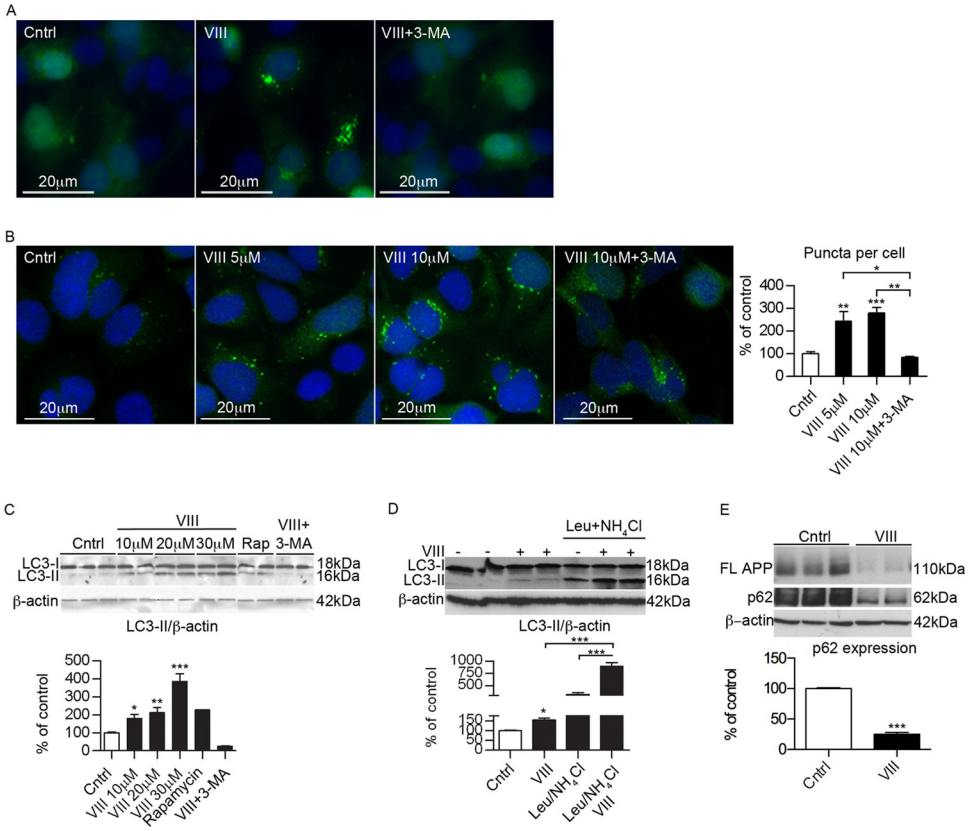

FIG 3 GSK3 inhibition induces autophagy pathway. (A) GSK3 inhibition induces autophagy. N2asw cells transfected with LC3-GFP cDNA were incubated for 18 h in serum-free media containing GSK3 inhibitor VIII (5 μM) and visualized with an epifluorescence microscope, and images were captured with a digital camera (×20 magnification). (B) HEK-293 cells stably transfected with LC3-GFP cDNA were incubated for 18 h in serum-free media containing GSK3 inhibitor VIII (5 and 10 μM) and visualized with Z-stacks from a Leica LAS AF SP5 confocal microscope (×63 optical magnification and 2.5× digital zoom). Quantification of punctum LC3 vesicles in those cells shows increased numbers with specific GSK3 inhibition. (C) Representative Western blot and quantification of LC3 in N2asw cells. Cells were incubated in serum-free media containing different concentrations of GSK3 inhibitor VIII, with or without the autophagy inhibitor 3-MA (500 μM) or the autophagy inducer rapamycin (20 μM) for 16 h. The intensity of the LC3-I and LC3-II bands was measured, and results are expressed as the ratio of LC3-II to total LC3 and LC3-II with respect to β-actin values ($n = 9$). (D) Autophagy flux was determined in N2asw cells by incubation with or without the inhibitors of lysosomal proteolysis, leupeptin (200 μM) and NH_4Cl (20 mM), for 4 h. The LC3-II/β-actin ratio was quantified and is represented ($n = 4$). (E) Representative Western blot and quantification of APP, p62, and β-actin of cell lysates from N2asw cells incubated for 18 h in serum-free media containing GSK3 inhibitor VIII (5 μM) or DMSO. Bars represent means ± SEM. Asterisks represent significant differences between control and treated cells (determined by one-way ANOVA, Tukey's *post hoc* test, or Student's *t* test). *, $P \leq 0.05$; **, $P \leq 0.01$; ***, $P \leq 0.001$.

knockdown of Atg5 attenuated the effect of GSK3 inhibition on APP (Fig. 4C).

Because it was previously demonstrated that autophagy is also effective in the clearance of APP-CTFs (37, 39), we determined whether inhibition of GSK3 reduced CTF levels as well. N2asw cells incubated with GSK3 inhibitor VIII showed decreased levels of CTF expression, and again this effect did not occur after silencing Atg5 expression (Fig. 4D). In addition, a reduction was observed in CHO cells permanently transfected with a C99 fragment after specific GSK3 inhibition (Fig. 4E).

An efficient autophagic process relies on the fusion of autophagosomes with lysosomes and activity of lysosomal hydrolases (32). Treatment with leupeptin (100 μM for 7 h) to inhibit lysosomal cysteine proteases significantly reduced the stimulated degradation of APP by GSK3 inhibition (Fig. 4F).

GSK3 inhibition induces lysosomal biogenesis. To determine whether GSK3 indeed affected the lysosomal system, we first performed immunofluorescence labeling of lysosomes with Lysotracker (Fig. 5A) or antibodies against LAMP-1 (Fig. 5C). Interestingly, GSK3 inhibition led to a striking increase in lysosomal staining. To further confirm our findings, electron microscopy studies were conducted on N2asw cells in the absence or presence of GSK3 inhibitor VIII (Fig. 5B). In agreement with the immunofluorescence results, we observed that GSK3 inhibition increased the number of lysosomes, in particular primary lysosomes (Fig. 5B).

To explore whether APP localization in lysosomes was altered after GSK3 inhibition, we performed double immunofluorescence labeling with APP and LAMP-1 antibodies. Costaining of LAMP-1 and APP revealed limited localization of APP and/or its CTFs in lysosomes. APP was mainly detected in juxtanuclear compartments, which is indicative for the Golgi complex. The low levels of APP in lysosomes might result from efficient degradation of APP in these compartments, which is consistent with previous reports (37) (Fig. 5C). Exposure to GSK3 inhibitor VIII increased accumulation of APP in lysosomes (Fig. 5C).

It was recently reported that the transcription factor EB (TFEB), which coordinates lysosomal formation (26), could func-

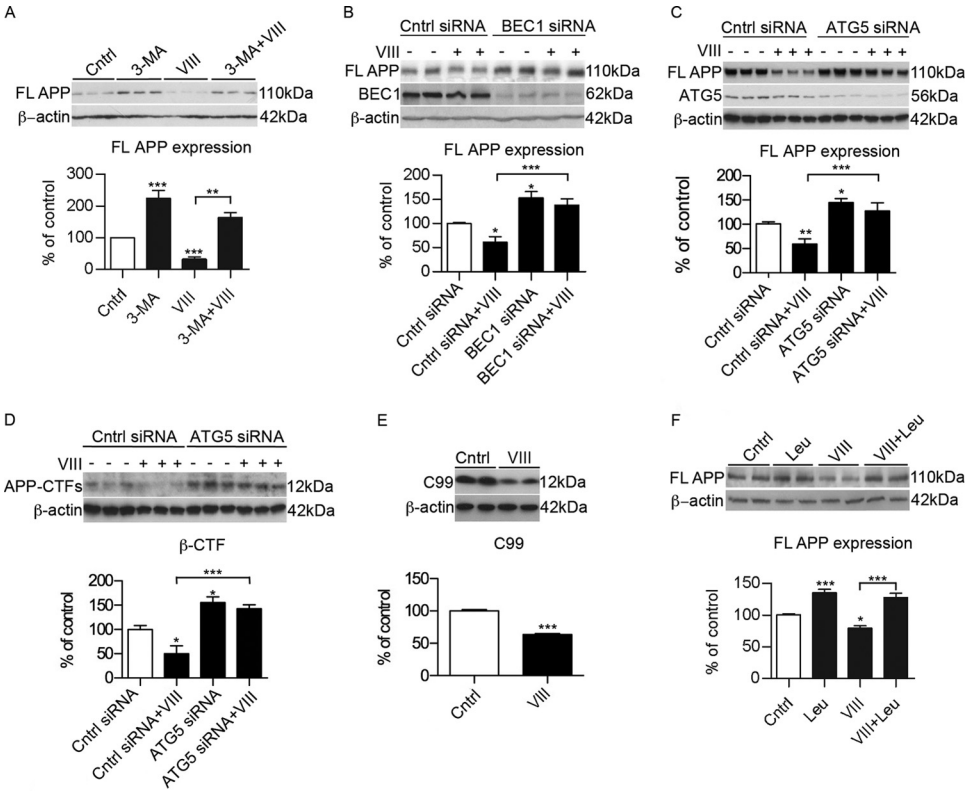

FIG 4 GSK3 inhibition induces APP and CTF degradation via autophagy/lysosomal pathway. (A) Representative Western blot and quantification of APP expression in N2asw cells incubated with the autophagy inhibitor 3-MA (500 μM) ($n = 4$). FL, full length. (B) Representative Western blot and quantification of full-length APP expression of N2asw cells transfected with the control or siRNA for BEC1 in the presence or absence of GSK3 inhibitor VIII (5 μM) ($n = 9$). (C) Representative Western blot and quantification of APP full-length expression of N2asw cells transfected with control siRNA or siRNA for ATG5 in the presence or absence of GSK3 inhibitor VIII (5 μM) ($n = 8$). (D) Representative Western blot and quantification of total CTFs of APP in N2asw cells transfected with control siRNA or siRNA for ATG5 treated with GSK3 inhibitor VIII (5 μM) ($n = 3$). (E) Representative Western blot and quantification of CTF (12 kDa) levels in CHO cells stably transfected with APP-C99 and treated with GSK3 inhibitor VIII (5 μM) ($n = 8$). (D) Inhibition of lysosomal proteases with 100 μM leupeptin resulted in increased stability of APP ($n = 4$). Bars represent means ± SEM. Asterisks represent significant differences between control and treated cells (determined by one-way ANOVA, Tukey's *post hoc* test, or Student's *t* test). *, $P \leq 0.05$; **, $P \leq 0.01$; ***, $P \leq 0.001$.

tion as a regulator of autophagy (33). Interestingly, GSK3 was identified as a potential kinase that phosphorylates TEFB (33). To investigate the relationship between GSK3 signaling and TFEB, we incubated N2asw cells transfected with Flag-tagged TFEB with GSK3 inhibitor VIII. Immunostaining of TFEB showed that GSK3 inhibition resulted in efficient TFEB nuclear translocation (Fig. 6A). In addition, we performed Western blotting of TFEB FLAG tag in nuclear extracts from cells treated with vehicle or with the inhibitor VIII, observing an increase of TFEB in the nuclear fraction when GSK3 was inhibited (Fig. 6B). The same results were obtained when we examined the endogenous TFEB nuclear translocation (Fig. 6C). To evaluate the relevance of TFEB on APP degradation, we decreased TFEB expression by siRNA in N2asw cells. Compared to control cells, silencing of TFEB attenuated the reduction in APP expression induced by GSK3 inhibition (Fig. 6D), supporting the hypothesis that TFEB nuclear translocation is essential to mediate the effects of GSK3 inhibition on APP degradation.

Taken together, these results suggest that the effect of GSK3 inhibition on APP involves enhanced lysosomal/autophagosomal activity due to an increase in lysosome biogenesis induced by TFEB transcriptional regulation.

DISCUSSION

Activation of GSK3 is found in a number of degenerative diseases, including AD, Parkinson's disease, Huntington's disease, schizophrenia, and diabetes (10, 13). Factors such as excessive caloric diet, hypertension, and aging, which have been associated with deficiency in insulin signaling and higher GSK3 activity, could affect the accumulation of aggregated proteins that are involved in neurodegenerative disorders, such as AD (17). Therefore, GSK3 has become an interesting target, since it links aging, metabolic disease, inflammation, protein aggregation, and cell death (13). Because brain GSK3 activity is increased in AD brains, this could have consequences for protein aggregation, Aβ generation, tau phosphorylation, and synaptic loss.

Over the last decade, there has been a lot of debate on the effects of GSK3 inhibition by LiCl as a therapeutic tool for AD based on studies using LiCl in different cell lines and animal models of AD. Some reports have shown beneficial effects of lithium in lowering Aβ load (23, 34, 35); however, there are many other studies that suggest that LiCl either has no effect or can aggravate Aβ production (6, 8). This inconsistency is likely due to the nonspecific action of LiCl. In this study, we tested two commercial cell-permeable and highly selective inhibitors of GSK3, with the advantage of

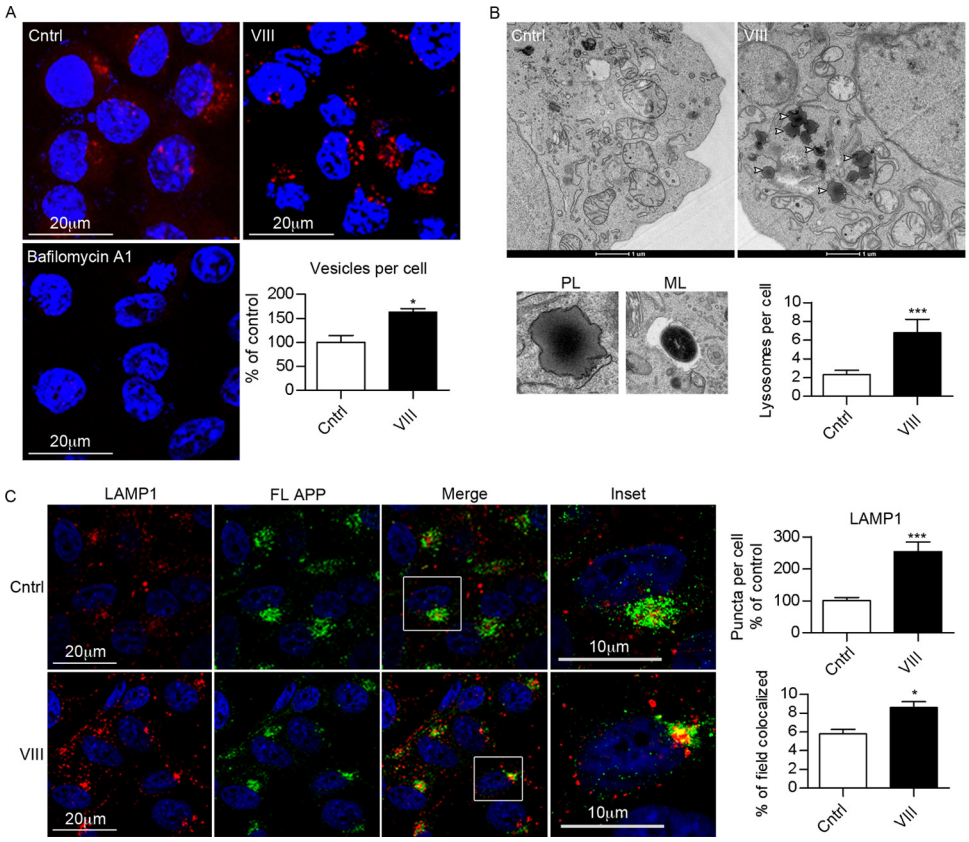

FIG 5 GSK3 inhibition increases lysosomal biogenesis. (A) Staining with Lysotracker in N2asw cells in the presence or absence of GSK3 inhibitor VIII (5 μM). The quantification of the number of vesicles per cell shows a clear increase in organelles with low internal pH after GSK3 inhibition. As an internal control, bafilomycin A1 (10 nM) was used. (B) Electron micrographs ×6500 of N2asw cells incubated for 18 h in deprived medium in the absence or presence of GSK3 inhibitor VIII (5 μM). Micrographs show representative pictures of primary lysosomes (PL), mature lysosomes (ML), and increased numbers of primary lysosomes in cells treated with GSK3 inhibitor. The total number of lysosomes per cell was counted for at least 30 cells/condition, and the average number of vesicles per cell is represented in the graphs. (C) Double immunostaining of APP (with antibody against its C terminus) and LAMP-1 in cells treated with DMSO or GSK3 inhibitor. Bars represent means ± SEM. Asterisks represent significant differences between control and treated cells (Student's *t* test). *, $P \leq 0.05$; ***, $P \leq 0.001$.

inhibiting at the micromolar range and showing no cross inhibition with the structurally related cyclin dependent kinases, which is characteristic of most GSK3 inhibitors (3), and compared them to LiCl. We observed a reduction in the levels of Aβ by specific GSK3 inhibitors but not by LiCl. We confirmed the results by reducing GSK3 levels using siRNA, which showed the same effects detected by pharmacological inhibition of GSK3.

Several hypotheses to explain the effects of GSK3 inhibition on APP processing have been raised. The first one supported the idea that GSK3α inhibition affected γ-secretase activity (23, 34). This hypothesis was interesting mainly because PS1 appears to bind β-catenin, which is one of the main targets of GSK3 (42). However, these results have not been reproduced by other groups, and we too were unable to detect differences in the APP intracellular domain (AICD) levels in a γ-secretase activity assay (data not shown).

On the other hand, other reports have attributed the decrease in Aβ by GSK3 inhibition to differences in APP phosphorylation, since a decrease in the levels of the phosphorylated form of APPThr668 in mice treated with lithium was noticed (24). The fact that GSK3 has multiple targets might explain the differences described in the literature regarding GSK3 inhibition on Aβ generation. In this study, we found a decrease in the levels of full-length APP and its CTFs by specific GSK3 inhibition, which was not due to changes in APP transcription. We further demonstrated that APP could be degraded at a higher rate when GSK3 is inhibited. We first explored the possibility that GSK3 induces an increase in proteasomal degradation and observed that inhibition of the proteasome partially reversed the effects of GSK3 inhibition. Because there is an active cross talk between proteasome and autophagic pathways in APP degradation (43), we analyzed the implications of autophagy on the effect of GSK3 inhibition. APP is internalized and processed through the lysosomal/endocytic pathway. It was demonstrated that autophagic vesicles contain Aβ and APP-CTFs (5, 16, 37, 39, 41). However, it remains controversial whether full-length APP is processed in autophagy. Recently, it was shown that APP can be found accumulated in autophagic compartments and that APP and its paralogue APLP1 are substrates for autophagy (16, 43). It also was found that BEC1 reduces cellular APP levels, and its deficiency alters APP metabolism (16). However, another study disagrees and showed no changes in APP after induction of autophagy by drugs such as rapamycin (5). Our results suggest that inhibition of autophagy by 3-MA and transfection with BEC1 siRNA reduced the effect of GSK3 inhibition on

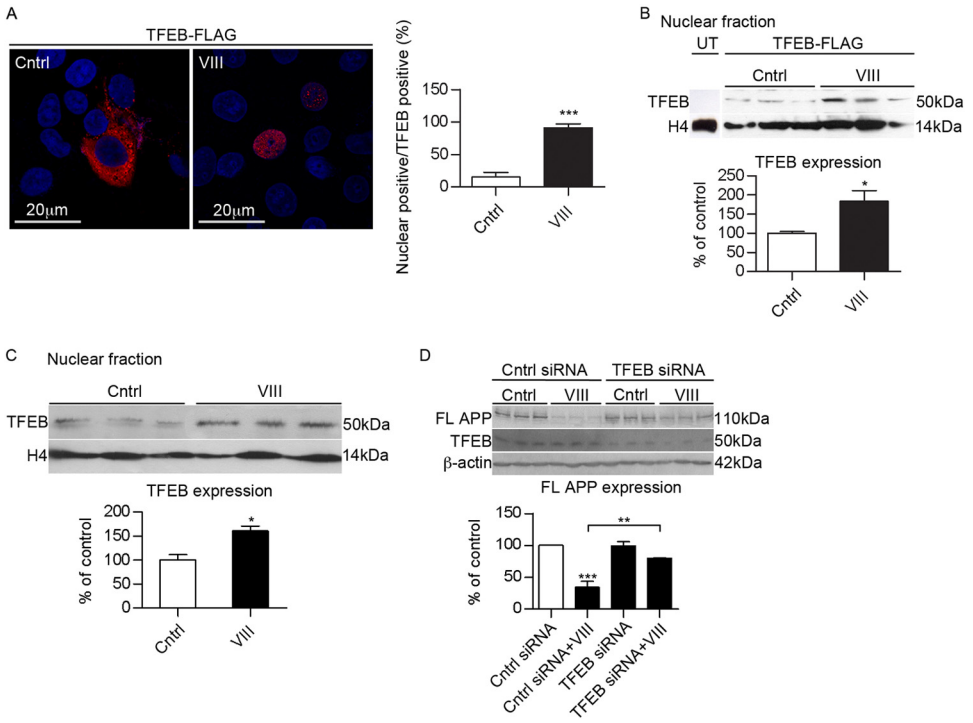

FIG 6 GSK3 regulates TFEB nuclear translocation. (A) Representative images and quantification of N2asw cells overexpressing TFEB cultured in DMSO or GSK3 inhibitor VIII (5 μM). TFEB nuclear localization was analyzed by Flag antibody and nuclear staining with 4′,6′-diamidino-2-phenylindole (DAPI) ($n = 4$). (B) Cells were subjected to subcellular fractionation, and the nucleus was blotted with an antibody against Flag. H4 was used as a nuclear marker ($n = 9$). UT, untransfected. (C) Endogenous TFEB staining shows increased TFEB nuclear trafficking in cells treated with GSK3 inhibitor ($n = 9$). (D) Representative Western blot and quantification of APP full-length expression of N2asw cells transfected with control siRNA or siRNA for TFEB in the presence or absence of GSK3 inhibitor VIII (5 μM) ($n = 9$) (determined by one-way ANOVA, Tukey's *post hoc* test, or Student's *t* test). *, $P \leq 0.05$; **, $P \leq 0.01$; ***, $P \leq 0.001$.

APP degradation, supporting the role of autophagy in APP processing. The concomitant inhibition of GSK3 and autophagy by ATG5 knockdown also precluded the GSK3-induced degradation of APP. Taken together, these experiments demonstrate the implication of autophagy in the GSK3-mediated effects on APP metabolism.

However, the role of GSK3 in autophagy induction has raised a lot of speculation. LiCl was reported to induce autophagy by an mTOR-independent mechanism via reduction of IMPase, lowering levels of IP3 (27). On the other hand, other groups have demonstrated that LiCl treatment inhibits mTOR (1, 12). Still, the effect of LiCl was thought to be mediated by a GSK3-independent mechanism (9), because there are indications that GSK3 activation inhibits the mTOR pathway (11, 15, 28). In contrast, other studies have reported that GSK3 inhibition induces autophagy by increasing Bif-1 levels (40) or have not found any change (25). The use of different cell lines, incubation times, GSK3 inhibitors, and culture conditions (with or without serum) could explain all of these different outcomes. Interestingly, our results show that specific GSK3 inhibition led to the activation of the lysosomal-autophagic network in neuronal cells by increasing the number of lysosomes. The master gene that regulates lysosomal biogenesis, TFEB, can be phosphorylated by GSK3 at serine 142. Intriguingly, TFEB phosphorylation at this particular serine by ERK2 affects the trafficking of this transcription factor, retaining TFEB in the cytosol (33). We show here that inhibition of GSK3 leads to the nuclear localization of TFEB, which results in stronger induction of the autophagic-lysosomal system. In addition, TFEB knockdown reversed the effects of GSK3 inhibition on APP levels. It is worth noting that the turnover of APP does not need to be mediated by autophagy, because APP can be directly targeted and processed in lysosomes (37).

Having in mind the complexity of GSK3, here we describe new mechanisms (proteasomal degradation, autophagic degradation, and lysosomal degradation not mediated by autophagy) by which GSK3 could regulate APP turnover. Most importantly, we show a new role of GSK3 as a regulator of lysosomal biogenesis which could have important consequences in neurodegenerative diseases, such as AD. Lysosomes contain hydrolases, such as cathepsins, which are involved in the degradation of Aβ. In fact, impaired clearance of autophagy and their contents by lysosomes might be an important factor in the development of the pathology (21). Alterations of GSK3 levels during aging and in AD therefore could have implications in the functionality of autophagic-lysosomal pathways and affect neuronal survival and Aβ levels. This is relevant because there is evidence of disturbed endosomal-lysosomal system function in AD (21).

ACKNOWLEDGMENTS

We thank Stefan Grimm (Imperial College London) for LC3-GFP cDNA, Andrea Ballabio (Theleton Institute of Genetics and Medicine, Naples, Italy) for TFEB cDNA, Gopal Thinakaran (University of Chicago) for N2asw cells, Satoru Funamoto (University of Doshisha, Japan) for the CHO-C99 cells, Sharon Tooze (Cancer Research UK, London, United Kingdom) for providing 293 cells permanently transfected with LC3-

GFP, and Christian Haass (University Munich) for the generous gift of antibody 5313.

M.S. received support from Imperial College London and Alzheimer's Research UK, and J.W. received support from the German Research Council (DFG; SFB645).

REFERENCES

1. **Aguib Y, et al.** 2009. Autophagy induction by trehalose counteracts cellular prion infection. Autophagy **5**:361–369.
2. **Bhat R, et al.** 2003. Structural insights and biological effects of glycogen synthase kinase 3-specific inhibitor AR-A014418 J. Biol. Chem. **278**: 45937–45945.
3. **Bhat RV, Budd Haeberlein SL, Avila J.** 2004. Glycogen synthase kinase 3: a drug target for CNS therapies. J. Neurochem. **89**:1313–1317.
4. **Blalock EM, et al.** 2004. Incipient Alzheimer's disease: microarray correlation analyses reveal major transcriptional and tumour suppressor responses. Proc. Natl. Acad. Sci. U. S. A. **101**:2173–2178.
5. **Boland B, et al.** 2010. Macroautophagy is not directly involved in the metabolism of amyloid precursor protein. J. Biol. Chem. **285**:37415–37426.
6. **Caccamo A, Oddo S, Tran LX, LaFerla FM.** 2007. Lithium reduces tau phosphorylation but not A beta or working memory deficits in a transgenic model with both plaques and tangles. Am. J. Pathol. **170**:1669–1675.
7. **Chan EYW, Kir S, Tooze SA.** 2007. siRNA screening of the kinome identifies ULK1 as a multi-domain modulator of autophagy. J. Biol. Chem. **282**:25464–25474.
8. **Feyt C, et al.** 2005. Lithium chloride increases the production of amyloid-beta peptide independently from its inhibition of glycogen synthase kinase 3. J. Biol. Chem. **280**:33220–33227.
9. **Fleming A, Noda T, Yoshimori T, Rubinsztein DC.** 2011. Chemical modulators of autophagy as biological probes and potential therapeutics. Nat. Chem. Biol. **7**:9–17.
10. **Frame S, Zheleva D.** 2006. Targeting glycogen synthase kinase-3 in insulin signalling. Expert Opin. Ther. Targets **10**:429–444.
11. **Fu L, et al.** 2009. Perifosine inhibits mammalian target of rapamycin signaling through facilitating degradation of major components in the mTOR axis and induces autophagy. Cancer Res. **69**:8967–8976.
12. **Heiseke A, Aguib Y, Riemer C, Baier M, Schätzl HM.** 2009. Lithium induces clearance of protease resistant prion protein in prion-infected cells by induction of autophagy. J. Neurochem. **109**:25–34.
13. **Hooper C.** 2007. Insulin signaling, GSK-3, heat shock proteins and the natural history of type 2 diabetes mellitus: a hypothesis. Metab. Syndr. Rel. Disord. **5**:220–230.
14. **Hooper C, et al.** 2007. Glycogen synthase kinase-3 inhibition is integral to long-term potentiation. Eur. J. Neurosci. **25**:81–86.
15. **Inoki K, et al.** 2006. TSC2 integrates Wnt and energy signals via a coordinated phosphorylation by AMPK and GSK3 to regulate cell growth. Cell **126**:955–968.
16. **Jaeger PA, et al.** 2010. Regulation of amyloid precursor protein processing by the Beclin 1 complex. PLoS One **5**:e11102. doi:10.1371/journal.pone.0011102.
17. **Jope RS, Johnson GV.** 2004. The glamour and gloom of glycogen synthase kinase-3. Trends Biochem. Sci. **29**:95–102.
18. **Katsouri L, Parr C, Bogdanovic N, Willem M, Sastre M.** 2011. PPARγ co-activator-1α (PGC-1α) reduces amyloid-β generation through a PPARγ-dependent mechanism. J. Alz. Dis. **25**:1–12.
19. **Klionsky DJ, et al.** 2008. Guidelines for the use and interpretation of assays for monitoring autophagy in higher eukaryotes. Autophagy **4**:151–175.
20. **Mizushima N, Yoshimori T.** 2007. How to interpret LC3 immunoblotting. Autophagy **3**:542–545.
21. **Nixon RA.** 2007. Autophagy, amyloidogenesis and Alzheimer disease. J. Cell Sci. **20**:4081–4091.
22. **Pei JJ, et al.** 1997. Distribution, levels, and activity of glycogen synthase kinase-3 in the Alzheimer disease brain. J. Neuropathol. Exp. Neurol. **56**:70–78.
23. **Phiel CJ, Wilson CA, Lee VM, Klein PS.** 2003. GSK-3alpha regulates production of Alzheimer's disease amyloid-beta peptides. Nature **423**: 435–439.
24. **Rockenstein E, et al.** 2007. Neuroprotective effects of regulators of the glycogen synthase kinase-3beta signaling pathway in a transgenic model of Alzheimer's disease are associated with reduced amyloid precursor protein phosphorylation. J. Neurosci. **27**:1981–1991.
25. **Rohatgi N, et al.** 2010. Therapeutic strategies to increase human β-cell growth and proliferation by regulating mTOR and GSK-3/β-catenin pathways. Open Endocrinol. J. **4**:40–54.
26. **Sardiello M, et al.** 2009. A gene network regulating lysosomal biogenesis and function. Science **325**:473–477.
27. **Sarkar S, et al.** 2005. Lithium induces autophagy by inhibiting inositol monophosphatase. J. Cell Biol. **170**:1101–1111.
28. **Sarkar S, et al.** 2008. A rational mechanism for combination treatment of Huntington's disease using lithium and rapamycin. Hum. Mol. Genet. **17**:170–178.
29. **Sastre M, Turner RS, Levy E.** 1998. X11 interaction with β-amyloid precursor protein modulates its cellular stabilization and reduces amyloid-β-protein secretion. J. Biol. Chem. **273**:22351–22358.
30. **Sastre M, et al.** 2001. Presenilin-dependent gamma-secretase processing of beta-amyloid precursor protein at a site corresponding to the S3 cleavage of Notch. EMBO Rep. **2**:835–841.
31. **Serenó L, et al.** 2009. A novel GSK-3beta inhibitor reduces Alzheimer's pathology and rescues neuronal loss in vivo. Neurobiol. Dis. **35**:359–367.
32. **Settembre C, Ballabio A.** 2011. TFEB regulates autophagy: an integrated coordination of cellular degradation and recycling processes. Autophagy **7**:1379–1381.
33. **Settembre C, et al.** 2011. TFEB links autophagy to lysosomal biogenesis. Science **332**:1429–1433.
34. **Su Y, et al.** 2004. Lithium, a common drug for bipolar disorder treatment, regulates amyloid-beta precursor protein processing. Biochemistry **43**: 6899–6908.
35. **Sun X, et al.** 2002. Lithium inhibits amyloid secretion in COS7 cells transfected with amyloid precursor protein C100. Neurosci. Lett. **321**: 61–64.
36. **Takashima A, et al.** 1996. Exposure of rat hippocampal neurons to amyloid beta peptide (25-35) induces the inactivation of phosphatidyl inositol-3 kinase and the activation of tau protein kinase I/GSK3beta. Neurosci. Lett. **203**:33–36.
37. **Tamboli IY, et al.** 2011. Sphingolipid storage affects autophagic metabolism of the amyloid precursor protein and promotes Abeta generation. J. Neurosci. **31**:1837–1849.
38. **Terwel D, et al.** 2008. Amyloid activates GSK-3beta to aggravate neuronal tauopathy in bigenic mice. Am. J. Pathol. **172**:786–798.
39. **Tian Y, Bustos V, Flajolet M, Greengard P.** 2011. A small-molecule enhancer of autophagy decreases levels of Abeta and APP-CTF via Atg5-dependent autophagy pathway. FASEB J. **25**:1934–1942.
40. **Yang J, et al.** 2010. GSK-3beta promotes cell survival by modulating Bif-1-dependent autophagy and cell death. J. Cell Sci. **123**:861–870.
41. **Yu WH, et al.** 2005. Macroautophagy–a novel beta-amyloid peptide-generating pathway activated in Alzheimer's disease. J. Cell Biol. **171**: 87–98.
42. **Zhang Z, et al.** 1998. Destabilization of beta-catenin by mutations in presenilin-1 potentiates neuronal apoptosis. Nature **395**:698–702.
43. **Zhou F, van Laar T, Huang H, Zhang L.** 2011. APP and APLP1 are degraded through autophagy in response to proteasome inhibition in neuronal cells. Protein Cell **2**:377–383.